ADVANCED ELECTRONIC MATERIALS

Supporting Information

for *Adv. Electron. Mater.*, DOI: 10.1002/aelm.201700395

Computation of Electronic Energy Band Diagrams for Piezotronic Semiconductor and Electrochemical Systems

*Lazarus N. German, Matthew B. Starr, and Xudong Wang**

Supporting Information

Computation of Electronic Energy Band Diagrams for Piezotronic Semiconductor and Electrochemical Systems

*Lazarus N. German, Matthew B. Starr, Xudong Wang**

Dr. M. B. Starr, L. N. German, Prof. X. D. Wang

Department of Materials Science and Engineering

University of Wisconsin-Madison

Madison, WI 53706, USA

E-mail: xudong.wang@wisc.edu

S1. Grand Scheme

Table S1. Summary of potential definitions as they are in Figure S1.

Potential *Vi*	Definition
V1	Work function of the metal
V2 [a)]	Potential at the metal/insulator interface
V3 [b)]	Potential at the insulator/n-type semiconductor (left side) interface
V4	Work function of the n-type semiconductor
V5	Potential at the n-type semiconductor (right side)/insulator interface
V6 [c)]	Potential at the insulator/p-type semiconductor (left side) interface
V7	Work function of the p-type semiconductor
V8	Potential at the p-type semiconductor (right side)/insulator interface
V9 [d)]	Potential at the insulator/solution interface
V10	Nernst potential of the solution

[a)](For a perfect metal and ideal heterojunction interface $V1=V2$); [b)] (For a metal/n-type semiconductor interface: $V3=V2$); [c)] (For a n-type semiconductor/p-type semiconductor interface: $V6=V5$); [d)] (p-type semiconductor/n-type semiconductor interface: $V9=V8$)

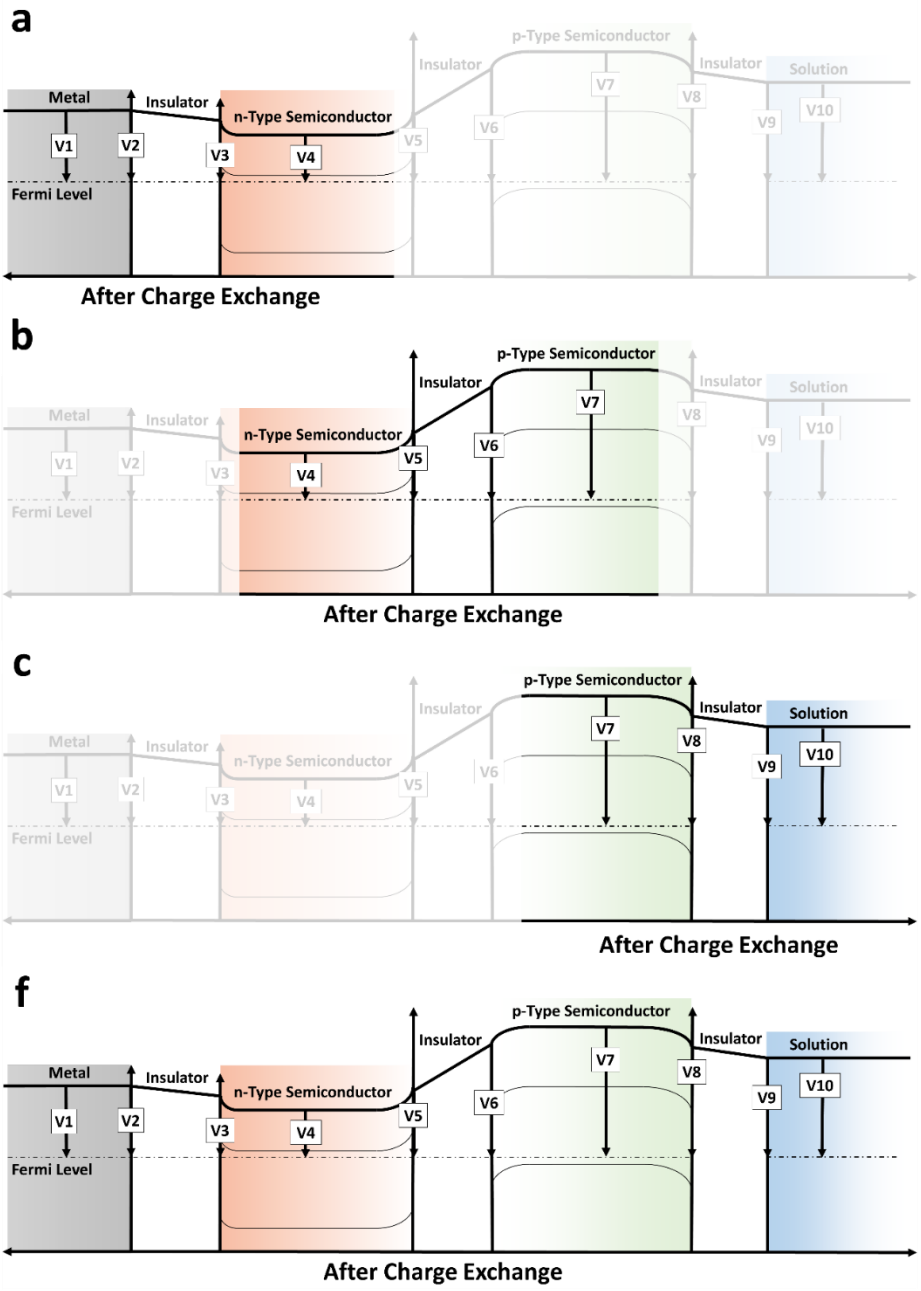

Figure S1. Grand scheme of the metal/insulator/n-type semiconductor/insulator/p-type semiconductor /insulator/solution after charge exchange and in equilibrium; discussed in the manuscript and subject of the full Mathematica code for calculating energy band diagrams. **a.**, **b.** and **c.** Schematics the metal/insulator/n-type semiconductor, n-type semiconductor/insulator/p-type semiconductor, and p-type semiconductor/insulator/solution heterojunctions, respectively.

These are the systems that are focused on separately within manuscript. **d.** Schematic of the full multi-junction.

S2. Review, Foundational Mathematics, and Calculations on Metal/Semiconductor System

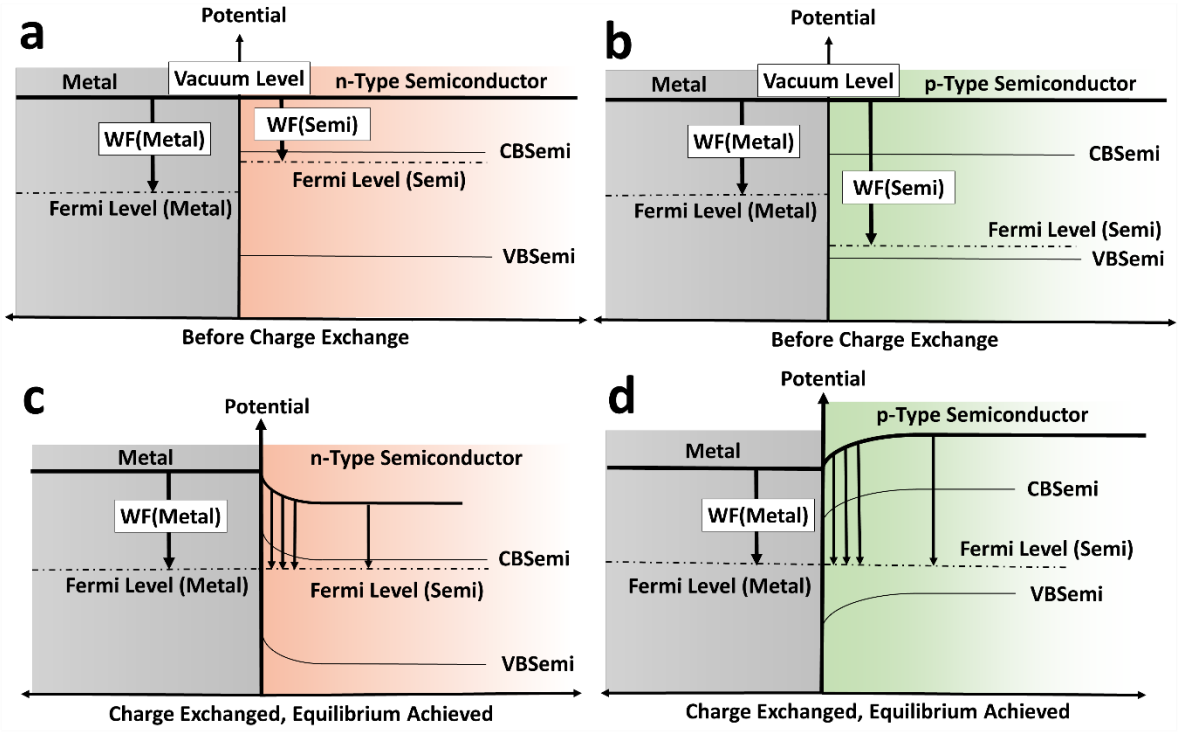

Figure S2. Representations of metal/semiconductor junctions. **a.** A metal n-type semiconductor junction. WF(Metal) and WF(Semi) are the work function of the metal and the work function of the semiconductor, respectively. CBsemi and VBsemi are the conduction and valence bands of the semiconductor, respectively. **b.** A metal p-type semiconductor junction. **c.** A schematic of the electrical potential profile across the metal/n-type semiconductor junction after equilibrium is established between the two materials. **d.** A schematic of the electrical potential profile across the metal/p-type semiconductor junction after equilibrium is established between the two materials.

A metal/semiconductor junction is often used to build Schottky solar cells, in which case it is appropriate to ask: To what depth does the band bending (or 'depletion region') extend within the semiconductor? It is only within this depletion length that photons absorbed by the semiconductor will contribute to a photocurrent. If one is building a scintillator or photomultiplier device out of a metal/semiconductor junction, an appropriate question might be: What is the magnitude of the electric field within the semiconductor as a function of distance? [1–5] The electric field within this region will impart acceleration to photoexcited charges and influence the impact ionization rate.

To quantitatively address these questions, we built a model of this single junction system. Before any charge flows between the metal and semiconductor, as depicted in Figure S2a and Figure S2b, no electric field exists between the two. Under ordinary conditions, as time passes, electrical charges in both materials will explore all of the electronic states available to them. If an electron goes from a high energy state to a low energy state, energy will be dissipated (i.e. spread out in space) and this will hinder the ability of the electron to return to its previous high-energy state.

Potential difference is a function of the charge, electrical permittivity, and distance over which the charge is distributed. The electrical permittivities of the system can be deduced from the materials chosen, but how does one determine how much charge has been transferred from one material to the next? Over what distance is that charge distributed?

Using a metal as one side of the heterojunction simplifies the matter significantly. Bulk metals have extremely high concentrations of free charges and the spacing in energy between any two occupiable electronic states is miniscule. As such, there will always be an abundance of charge ready to accumulate or deplete at the surface of a metal incident to an electric field. Here, 'surface' means a length scale on the order of an angstrom. Regardless of charge magnitude, any potential

drop within the metal over this distance is going to be relatively small—indeed negligible—when compared to the very poor electrical field screening capacity associated with semiconducting materials. Thus, the entirety of the potential drop in the metal/semiconductor junction (which is equal to the work function difference between the two materials) will occur within the semiconducting material. This is graphically demonstrated in **Figure S3**a, where V_1 is the potential within the bulk of the metal, V_2 is the potential at the interface between the metal and semiconductor, and V_3 is the potential within the bulk of the semiconductor. In this case, the potential energy change within the metal is $V_{MetalDrop} = V_1 - V_2 = 0$, and the potential energy within the semiconductor is $V_{SemiDrop} = V_2 - V_3 = V_1 - V_3$.

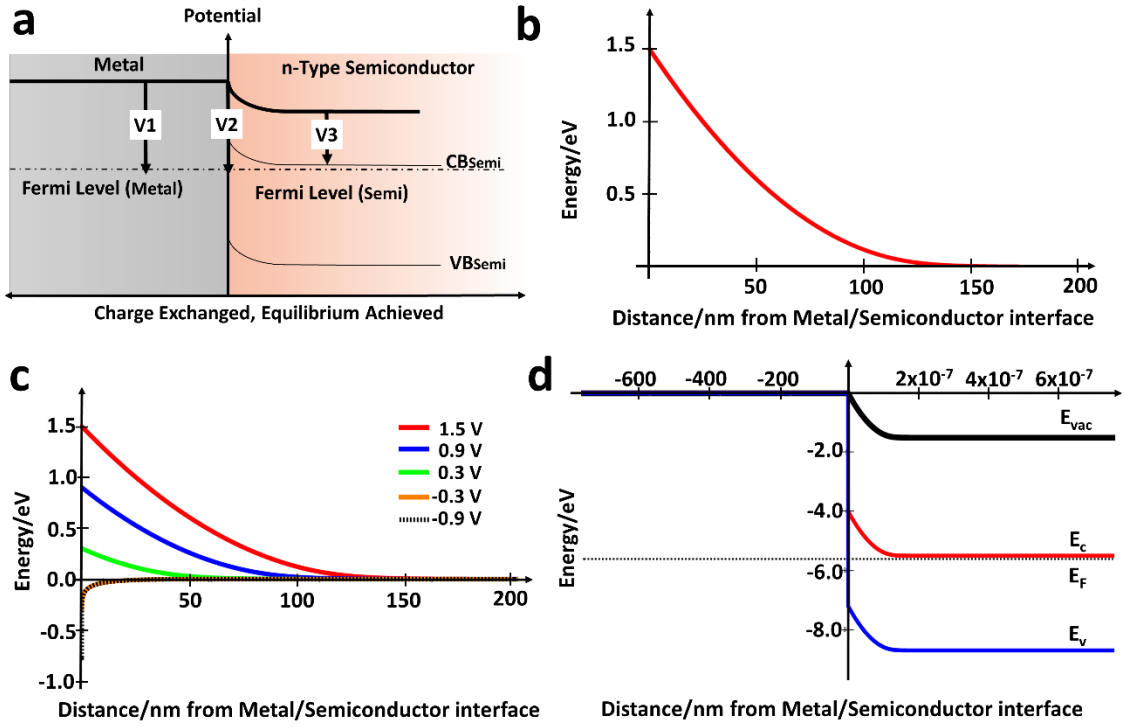

Figure S3. Calculating the electrical potential profile that results from establishing equilibrium at a metal/n-type semiconductor junction. **a.** A metal/n-type semiconductor junction. V1, V2 and V3 represent the work function in the bulk of the metal, at the metal/semiconductor interface, and in the bulk of the semiconductor, respectively. **b.** Result of the electrical potential profile calculated

at the metal/semiconductor interface. **c.** Multiple electrical potential profiles at the metal/semiconductor interface that result from varying the work function difference between the metal and semiconductor. The spatial extent of the potential profile is greater when there is a positive voltage difference between the two work functions than when there is a negative potential difference because the n-type semiconductor is more easily able to accumulate electrons (negative charges) than holes (pseudo-positive charges). **d.** An equilibrium energy band diagram of the metal/n-type semiconductor interface generated for a work function difference of 1.5 V.

To calculate the potential profile in the heterojunctions, the potential energy change $V_{SemiDrop}$ must now be related to the length scale of the depletion region. Knowing that we must relate the potential at the semiconductor junction to the amount of net charge in the semiconductor over some distance *x*, we begin with the one-dimension Poisson Equation:

$$\rho(x) = -\varepsilon_r \varepsilon_0 \frac{\mathrm{d}^2 \varphi(x)}{\mathrm{d}x^2} \tag{S1}$$

where $\rho(x)$ is the charge density at position *x*, ε_r is the relative electrical permittivity of the medium, ε_0 is the permittivity of vacuum, and $\phi(x)$ is the potential at distance *x* from the interface.

There are four possible sources of charge inside the semiconductor: 1) mobile electrons (*n*) due to thermal excitation and dopant atoms, 2) mobile holes (*p*) due to thermal excitation and dopant atoms, 3) negatively charged ionized dopant atoms (N_A), 4) positive charged ionized dopant atoms (N_D).

$$\rho(x) = n + p + N_A + N_D = -\varepsilon_{Semi} \varepsilon_0 \frac{d^2 \varphi(x)}{dx^2} \tag{S2}$$

Or, after rearrangement:

$$\frac{d^2 \varphi(x)}{dx^2} = \frac{n+p+N_A+N_D}{-\varepsilon_{Semi} \varepsilon_0} \tag{S3}$$

The concentration of ionized dopant atoms, N_A and N_D, in Equation (S3) can have a spatial and thermal dependence but pragmatically they can be taken as constant. Here, the relative permittivity of the medium ε_r has been further specified as the relative permittivity of the semiconductor, ε_{Semi}. The concentration of mobile electrons (n) and holes (p) within in the semiconductor depend sensitively on the local potential in the following way: [10,11,23]

$$n = n_b exp[\frac{-z_n e\varphi(x)}{kT}] \quad \text{(S4)}$$

and

$$p = p_b exp[\frac{-z_p e\varphi(x)}{kT}] \quad \text{(S5)}$$

where n_b and p_b are the concentration of electrons and holes in the bulk of the semiconductor, respectively, the location potential ($\phi(x)$) is constant, z_n [-1] and z_p [+1] are the charge signs of the electron and hole, respectively. e is the magnitude of elementary charge [C], k is the Boltzmann constant [J K^{-1}] and T is the absolute temperature [K]. Combining Equation (S3), (S4), and (S5), yields the following expression:

$$\frac{\mathrm{d}^2\varphi(x)}{\mathrm{d}x^2} = \frac{n_b \exp[\frac{-z_n e\varphi(x)}{kT}] + p_b \exp[\frac{-z_p e\varphi(x)}{kT}] + N_A + N_D}{-\varepsilon_{Semi}\varepsilon_0} \quad \text{(S6)}$$

The bulk concentrations of electrons (n_b) and holes (p_b) depend both on the carrier density that is thermally excited over the bandgap of the semiconductor and those contributed by the dopant species. In a semiconductor with a moderate bandgap (e.g. 1.2 eV or higher) and dopant density ($1 * 10^{16}\mathrm{cm}^{-3}$), the charge carriers contributed by the dopant atoms will be several orders of magnitude greater than those contributed by thermal excitation across the bandgap. For the case of an n-type semiconductor (e.g. Figure S1a), that would mean that $n_b = N_D$, and for a p-type semiconductor (e.g. Figure S1b), $p_b = N_A$.

If the semiconductor is not degenerately doped, the concentration of electrons and holes will obey the mass-action law:[6,7]

$$n_b p_b = {n_i}^2 \tag{S7}$$

where the bulk mobile electron and hole concentration sum to the square of the intrinsic. Thermally excited charge concentration n_i. n_i is expressed as follows:

$$n_i = N_C \exp[-\frac{E_g}{2kT}] \tag{S8}$$

where N_C is the density of states in the conduction band of the semiconductor [cm^{-3}] and E_g is the bandgap of the semiconductor [eV]. Thus, in the case of a n-type semiconductor with no p-type doping:

$$n_b = N_D, N_A = 0 \tag{S9}$$

and

$$p_b = \frac{{n_i}^2}{n_b} = \frac{{n_i}^2}{N_D} = \frac{\left(N_C \exp\left[-\frac{E_g}{2kT}\right]\right)^2}{N_D} \tag{S10}$$

If we were looking at the case of a p-type semiconductor with no n-type doping, then:

$$p = N_A\ ,\ N_D = 0 \tag{S11}$$

and

$$n_b = \frac{{n_i}^2}{p_b} = \frac{{n_i}^2}{N_A} = \frac{(N_V \exp\left[-\frac{E_g}{2kT}\right])^2}{N_A} \tag{S12}$$

where N_V is the density of states in the valence band.

To express the relationship between electrical potential and charge density within the n-type semiconductor featured in Figure S1a, we combine Equation (S6), (S9) and (S10):

$$\frac{\mathrm{d}^2\varphi(x)}{\mathrm{d}x^2} = \frac{N_D \exp\left[\frac{-z_n e\varphi(x)}{kT}\right] + \frac{\left(N_C \exp\left[-\frac{E_g}{2kT}\right]\right)^2}{N_D} \exp\left[\frac{-z_p e\varphi(x)}{kT}\right] + N_A + N_D}{-\varepsilon_{Semi}\varepsilon_0} \quad \text{(S13)}$$

If Equation (S13) can be integrated twice then it would be an expression for the entire potential profile $\phi(x)$, and thus band bending, throughout the semiconductor. The first integration is achieved by recognizing that far from the metal/semiconductor interface the potential is the bulk potential of the semiconductor ($\phi(\infty) = 0$) and the gradient in potential (i.e. the electrical field) is zero ($\frac{\mathrm{d}\varphi(\infty)}{\mathrm{d}x} = 0$). Integrating Equation (S13) with these boundary conditions gives us:[23]

$$\frac{\mathrm{d}\varphi(x)}{\mathrm{d}x} = -\left\{\frac{2kT}{\varepsilon_{Semi}\varepsilon_0}\left[N_D \exp\left[\frac{-z_n e\varphi(x)}{kT}\right] + \frac{N_C^2 \exp\left[-\frac{E_g}{kT}\right]}{N_D} exp\left[\frac{-z_p e\varphi(x)}{kT}\right] - \frac{eN_D z_{N_D}\varphi(x)}{kT} - \left(N_D + \frac{N_C^2 \exp\left[-\frac{E_g}{kT}\right]}{N_D}\right)\right]\right\}^{\frac{1}{2}} \quad \text{(S14)}$$

Equation (S14) can be integrated again if a boundary condition is known, though the result may not always be analytic and thus a numerical solver must be used to visually represent the result. The boundary condition used in Equation (S14) is the fact that at the interface between the metal and semiconductor ($x = 0$) the potential $\phi(x)$ is at a maximum and takes the value of the full potential difference between semiconductor and metal, as seen in Figure 2a:

$$\varphi(0) = V_{SemiDrop} = V_2 - V_3 = V_1 - V_3 \quad \text{(S15)}$$

The general form of the output function *PontentialProfileCurve1*[x], within the bounds that is interpolated, will be that of Figure S3b. To automatically convert these potential curves into band diagrams is relatively straight forward: define the regions of interest and plot the work functions of each region together. For the single metal/semiconductor heterojunction example:

- when $x \leq 0$: the potential $\phi = V_1$,

- when x is within the depletion region: $\phi = V_1 - (PotentialProfileCurve1[x] - V_{SemiDrop})$,
- when $x \geq$ depletion layer thickness: $\phi = V_3$.

To determine how far along x, the depletion region extends, find the root of $PotentialProfileCurve1[x]$. It is important to note that the calculated length over which the depletion region extends) can be much larger than is physically relevant. This length scale is calculated by determining when the electrical potential gradient (i.e. electric field) is equal to zero within the vicinity of the interface. The function describing the electrical potential gradient is exponential and thus may maintain a value that is extremely small over a long distance before it becomes zero. The process described above is necessary to compute and generate an accurate band diagram but a more pragmatic length scale is the region over which the potential within the vicinity of the metal/semiconductor junction deviates significantly ($>kT$) from equilibrium (bulk semiconductor) potential values (V_3).

With the integratation of Equation (S14), we can now easily plot the electrical potential profile within the vicinity of the metal/semiconductor heterojunction as a function of metal work function V_1 (or alternatively, applied potential), and semiconductor dopant density N_D, work function V_3, and electrical permittivity ε_{Semi}. Figure S3c depicts the electrical potential profiles of a metal/semiconductor junction under various values of metal work functions (V_3), which is also equivalent to varying the potentials applied to the metal electrode. Figure S3d is the output for a work function difference between the metal and semiconductor of 1.5 eV.

S3. Mathematics for p-n and p-i-n Junctions

Throughout the manuscript, we focus on three general heterojunctions: metal/insulator/n-type semiconductor (Figure S1a), n-type semiconductor/insulator/p-type semiconductor (Figure S1b), and p-type semiconductor/insulator/solution (Figure S1c). We label potentials within the

model at materials interfaces and relevant bounds (i.e. where work functions are approximately bulk values) as *V1, V2, V3,…,V10* for our so-called 'grand' multi-junction: metal/insulator/n-type semiconductor/insulator/p-type semiconductor /insulator/solution (Figure S1d).

Unlike the metal/semiconductor junction analyzed previously, the total potential drop $V_7 - V_4$ will not happen within a single side of the junction. Instead, the potential change on both sides of the heterojunction will sum to the work function difference between the two semiconductors:

$$V7 - V4 = (V7 - V6) + (V6 - V5) + (V5 - V4) \quad \text{(S16)}$$

V_4 and V_7 are known quantities; V_5 and V_6 are unknown but linearly related to each other via the thickness and electrical permittivity of the second insulating layer:

$$V5 = V6 - ElectricFieldInInsulator2 * dIns2 \quad \text{(S17)}$$

where *dIns2* is thickness of the insulating layer between the two semiconductors and *ElectricFieldInInsulator2* is the electric field in this insulating layer, given by:

$$ElectricFieldInInsulator2 = \frac{qsemiconductor1Rightperarea}{epsIns2} = -\frac{qsemiconductor2Leftperarea}{epsIns2} \quad \text{(S18)}$$

where *qsemiconductor1Rightperarea* and *qsemiconductor2Leftperarea* are the charge densities in the two semiconductors at the semiconductor/insulator/semiconductor junction.

Without any piezoelectric of ferroelectric charge density in the interface, all charge at the interface of semiconductor2 must have come from semiconductor1 during the equilibration process. The charge density in semiconductor1 at the interface, *qsemiconductor1Rightperarea*, is given by:

$$qsemiconductor1Rightperarea = epsSemi1 * ElectricFieldInRightSemi1 \quad \text{(S19)}$$

where *epsSemi1* is the permittivity of semiconductor1, and *ElectricFieldInRightSemi1* is the electric field at the interface within semiconductor1 and thus is given by:

$$E(ElectricFieldInRightSemi1) =$$

$$-\left\{\frac{2kT}{\varepsilon_{Semi1}\varepsilon_0}\left[N_{D,Semi1}\exp\left[\frac{-z_n(V_5-V_4)}{kT}\right]\right.\right.$$
$$+\frac{N_{C,Semi1}^2\exp\left[-\frac{E_{g,Semi1}}{kT}\right]}{N_{D,Semi1}}\exp\left[\frac{-z_p e(V_5-V_4)}{kT}\right]$$
$$-\frac{eN_{D,Semi1}z_{N_{D,Semi1}}(V_5-V_4)}{kT}$$
$$\left.\left.-\left(N_{D,Semi1}+\frac{N_{C,Semi1}^2\exp\left[-\frac{E_{g,Semi1}}{kT}\right]}{N_{D,Semi1}}\right)\right]\right\}^{\frac{1}{2}} \quad \text{(S20)}$$

The electric field in semiconductor2 at the interface is due to the same charge density but as a function of its own material parameters:

$$E(ElectricFieldInLeftSemi2) =$$
$$-\left\{\frac{2kT}{\varepsilon_{Semi2}\varepsilon_0}\left[N_{D,Semi2}\exp\left[\frac{-z_n(V_7-V_6)}{kT}\right]\right.\right.$$
$$+\frac{N_{C,Semi2}^2\exp\left[-\frac{E_{g,Semi2}}{kT}\right]}{N_{D,Semi2}}\exp\left[\frac{-z_p e(V_7-V_6)}{kT}\right]$$
$$-\frac{eN_{D,Semi2}z_{N_{D,Semi2}}(V_7-V_6)}{kT}$$
$$\left.\left.-\left(N_{D,Semi2}+\frac{N_{C,Semi2}^2\exp\left[-\frac{E_{g,Semi2}}{kT}\right]}{N_{D,Semi2}}\right)\right]\right\}^{\frac{1}{2}} \quad \text{(S21)}$$

Recognizing that the charge density in both materials must be equal, Equation (S19), (S20) and (S21) can be combined into the following expression:

$$E(ElectricFieldInRightSemi1) * epsSemi1 =$$

$$E(ElectricFieldInRightSemi2) * epsSemi2 \tag{S22}$$

Or

$$\begin{aligned}
&-\left\{\frac{2kT}{\varepsilon_{Semi1}\varepsilon_0}\left[N_{D,Semi1}\exp\left[\frac{-z_n(V_5-V_4)}{kT}\right]\right.\right. \\
&\quad + \frac{N_{C,Semi1}^2\exp\left[-\frac{E_{g,Semi1}}{kT}\right]}{N_{D,Semi1}}\exp\left[\frac{-z_p e(V_5-V_4)}{kT}\right] \\
&\quad - \frac{eN_{D,Semi1}z_{N_{D,Semi1}}(V_5-V_4)}{kT} \\
&\quad \left.\left. - \left(N_{D,Semi1} + \frac{N_{C,Semi1}^2\exp\left[-\frac{E_{g,Semi1}}{kT}\right]}{N_{D,Semi1}}\right)\right]\right\}^{\frac{1}{2}} = \\
&-\left\{\frac{2kT}{\varepsilon_{Semi2}\varepsilon_0}\left[N_{D,Semi2}\exp\left[\frac{-z_n(V_7-V_6)}{kT}\right]\right.\right. \\
&\quad + \frac{N_{C,Semi2}^2\exp\left[-\frac{E_{g,Semi2}}{kT}\right]}{N_{D,Semi2}}\exp\left[\frac{-z_p e(V_7-V_6)}{kT}\right] \\
&\quad - \frac{eN_{D,Semi2}z_{N_{D,Semi2}}(V_7-V_6)}{kT} \\
&\quad \left.\left. - \left(N_{D,Semi2} + \frac{N_{C,Semi2}^2\exp\left[-\frac{E_{g,Semi2}}{kT}\right]}{N_{D,Semi2}}\right)\right]\right\}^{\frac{1}{2}}
\end{aligned} \tag{S23}$$

If materials properties in Equation (S23) are known, then Equation (S17) gives us the means to relate *V5* to *V6*. All that is left for establishing a potential profile of the semiconductor/insulator/semiconductor junction is to find the value of V_5 in Equation (S23) for

which both sides equate. The majority of the expressions like this that one encounters need to be solved numerically, which can be done using the FindRoot command in Mathematica.

S3.1. p-n Junction Schematics and Calculated Figures

The reader might notice that we do not subsequentially include junctions that exclude an intermediate insulator after examination of the metal/semiconductor (Figure 1 in manuscript)—we provide those here. In particular, a p-n junction (Figure S4a-b) for the n-type/insulator/p-type junction, and a semiconductor-solution junction for the p-type/insulator/solution have been omitted from the manuscript. This simply allows us to explore more pathways at a time for each of these junctions, and to reflect real or non-ideal physical structures. Here, we provide calculated potential profiles and energy band diagrams for a p-n junction as functions of the dopant density in the semiconductors (Figure S4c-d) and work function difference between the n- and p-type semiconductors (Figure S4e-g). Note for the band diagrams in Figure S4f and g: the conduction and valence bands for the n-type semiconductor reflect that of ZnO while the p-type represents a hypothetical semiconductor where the relative positions for E_F, E_{CB}, and E_{VB} remain constant. The positions of E_F, E_{CB}, and E_{VB} for the p-type semiconductor change relative to E_{vac} depending on the given conditions (i.e. $V7 - V4$).

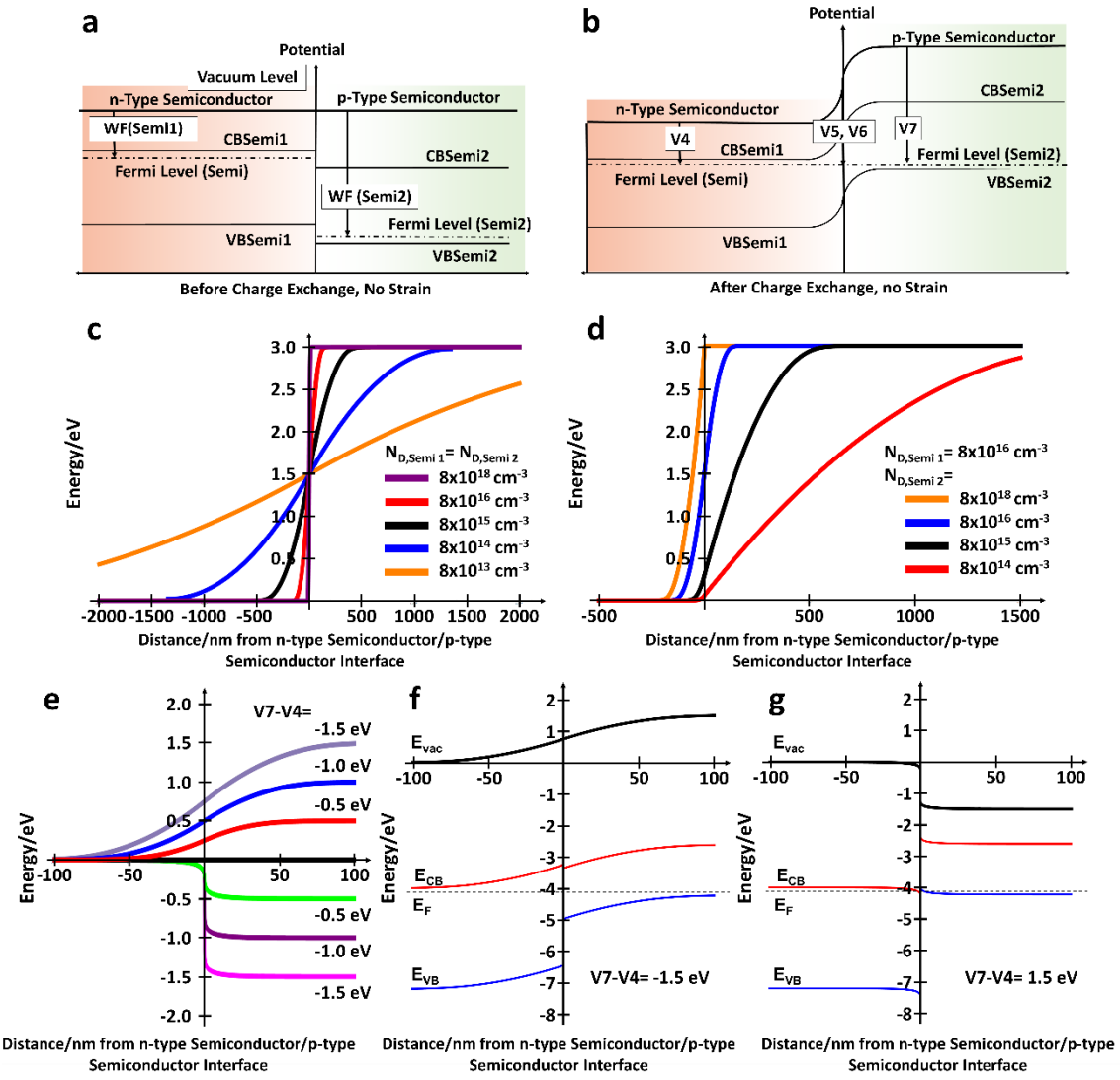

Figure S4. Effects of dopant density and work function difference in a p-n junction. **a.** and **b.** schematics of the p-n junction before and after equilibrium is achieved. **c.** potential profile when the n- and p-type semiconductors have equal dopant concentrations. **d.** potential profile as a function of n-type dopant concentration with constant p-type dopant concentration. The higher the dopant concentration in the semiconductor, the more effective it is at supplying charge to compensate for the work function difference; depletion width decreases as dopant concentration increases. **e.** potential profile as a function of work function difference. **f.** and **g.** are the energy

band diagrams for work function difference of -1.5 eV (V7<V4) and 1.5 eV (V7>V4) with respect to vacuum level, respectively.

S4. Solid-Electrolyte Junctions

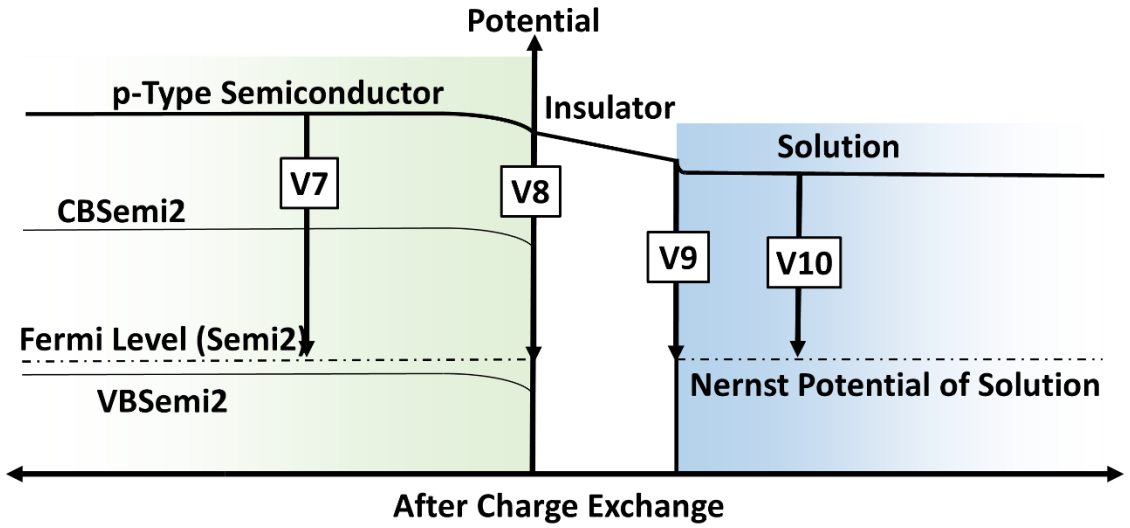

Figure S5. Schematic of the semiconductor/insulator/solution heterojunction after equilibrium is achieved.

Discussion of ion packing at solid/solution interface: If we model the hydrated ions as hard spheres, then the maximum packing density possible for ions in the solution is the close packing structure (**Figure S6**).

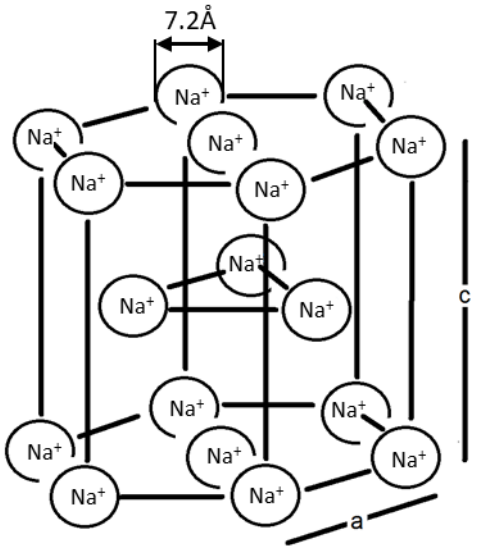

Figure S6. Proposed hexagonal close-packed structure of hydrated Na^+ ions, taken as an example.

We first calculate the total atomic density of charged species at the solid-solution interface:

$$n_i = n_i^0 \left[e^{\left(\frac{-z_i\, e\, \phi(x)}{kT}\right)} \right] \tag{S24}$$

where i = OH^-, H^+, Na^+ for our system (1M aqueous NaOH). In our analysis, Equation (S24) is used for the ionic densities in solution the same way Equation (S4) and (S5) are used for electron and hole densities in semiconductors.

We now consider the diameter of hydrated ions (d_{ion}) and the resultant density in a hexagonal close-packed (hcp) structure. We choose the ion that has the largest hydrated ionic diameter and concentration and determine the close-packed density of that ion. The atomic packing factor (APF) of close-packed structures is given by:

$$APF_{hcp} = \frac{N_{ion}\, V_{ion}}{V_{hcp}} = \frac{\sqrt{2}}{6}\pi \tag{S25}$$

N_{ion} is the number of *hydrated* ions with hydrated ionic volumes of V_{ion} contained within hcp unit cell of volume V_{hcp}. With $V_{ion} = \frac{\pi}{6} d_{ion}^3$, we have the hydrated ionic packing density:

$$n_{ion} = \frac{N_{ion}}{V_{hcp}} = \frac{\sqrt{2}}{d_{ion}^3} \tag{S26}$$

Referring back to Figure S6 we take hydrated Na^+ ions as an example, each with a hydration diameter (d_{Na^+}) of 7.2 Å, we get the maximum 3D possible packing density possible is given by:[8]

$$n_{\max} = \frac{\sqrt{2}}{d_{Na^+}^3} = 3.8 * 10^{27}\ \frac{\text{ions}}{\text{m}^3} \tag{S27}$$

Thus, the sum total of all ion concentrations at the closest approach to the 2D charged layer must be equal to or less than this atomic density.

$$\sum_i n_i \leq 3.8 * 10^{27}\ \frac{\text{ions}}{\text{m}^3} \tag{S28}$$

If the calculated atomic density at the solution interface is less than $\sum n_i$ then the system remains at least physically reasonable. If the atomic density calculated at the solution interface is greater than $\sum n_i$, then the solution has a charge density greater than a close-packed atomic density and this is an unphysical result.

The charge density is determined by the electrical potential, thus there is a critical potential ($V_{\max}$) at which ions in solution will accumulate to a density equal to n_{max}, and any potential greater than $V_{\max}$ will result in an unphysical value.

$$\sum_i \left(n_i^0 \left[e^{\left(\frac{-z_i e V max}{kT}\right)} \right] \right) = n_{\max} \tag{S27}$$

where the left side of the expression is the familiar one describing the charge density in solution at point x as a function of the potential at point x, and the right side is the maximum packing density determined by Equation (S26).

If the charge density found at the solid-solution interface is below the calculated (i.e. $\sum n_i \leq n_{\max}$*), then the following step may be skipped.*

This step is a means of determining at what potential ($V_{\max}$) is necessary at the solution interface to obtain our maximum charge density obtained above. $V_{\max}$ is the maximum potential that corresponds to a physically meaningful charge density in solution, but if our calculation produces a potential at the interface greater than $V_{\max}$, we must invoke a physically meaningful mechanism to reduce the potential at the interface to or below V_{max}. The mechanism we invoke is a charged Stern layer with a charge density σ^S. A charged Stern layer might take the form of a close-packed, 2D hexagonal array of charged hydrated ions (Figure S7).

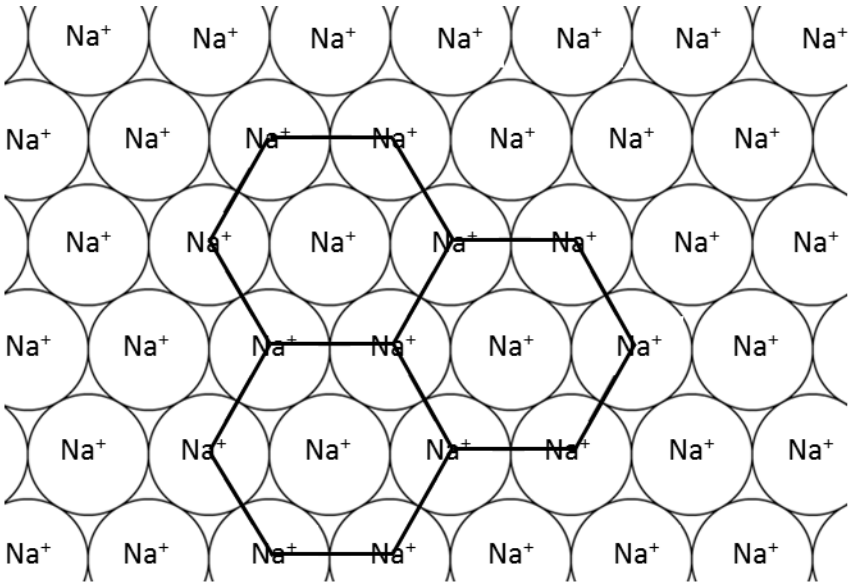

Figure S7. A 2D array of Na^+ ions demonstrating a densely packed array forming a Stern layer at the solid-liquid interface.

The charge density necessary in the Stern layer for reducing the potential at the interface to V_{max} can be determined as follows:

If the charge density at the interface is higher than the maximum charge density allowed then the potential at the interface (*V9* in Figure S1) is greater than V_{max}. Under these conditions, we assume that our hexagonal close-packed Stern layer will form at the interface (Figure S6 and S7). This sheet of hydrated ions will reduce the potential between the interface and the solution so that the potential value becomes equal to V_{max} (**Figure S8**).

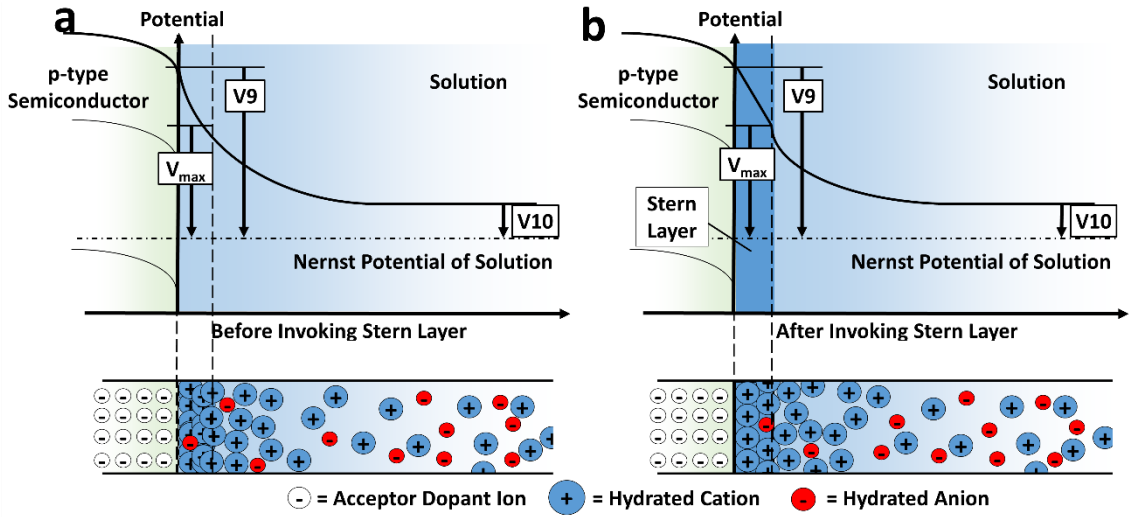

Figure S8. Schematic illustrating an **a.** unphysical accumulation of hydrated ions at a semiconductor-solution interface, taken as an example. Since *V9* > V_{max}, there is an ion concentration near the interface that exceeds the physical limitations given for the dense packing of hydrated ions. **b.** shows the results of invoking a Stern layer wherein close-packing of hydrated ions lowers the potential near the interface from *V9* to V_{max} and allows a physical result for the ionic diffuse layer in the solution.

To obtain the value of V_{max}, we simply find the solution to Equation to S27. For example, we solve the following equation for aqueous NaOH:

$$n^0_{OH^-} e^{\left(\frac{e\,Vmax}{kT}\right)} + n^0_{Na^+} e^{\left(\frac{-e\,Vmax}{kT}\right)} + n^0_{H^+} e^{\left(\frac{-e\,Vmax}{kT}\right)} = n_{max} \qquad \text{(S28)}$$

Though the left side of the equation includes concentration terms of all ionic species, we may still use the n_{max} calculated for Na^+ since it gives us the smallest limiting density for close-packed hydrated ions necessary for a Stern layer. It is also important to note that all accumulating ions that make up the Stern layer do not necessarily have to be the same charge. In fact, there will be some minority ions (e.g. OH^- ions if Na^+ ions dominate the Stern layer) within the Stern layer as a balance between diffusional forces and electric field.

If physicality broke down because the potential change in the solution |*V10-V9*| > $|V_{max}|$, then we must determine what amount of charge to place in and outside the Stern layer in the solution. We do this by solving for the electric field strength ($\frac{d\phi_{Sol,Test}}{dx}$) necessary to create V_{max} in the solution, and subtract this value from the actual of the electric field strength (corresponding to the total solution charge density $q_{Solution}$) we find via our standard procedure outlined ($\frac{d\phi_{Solution}}{dx}$):

- $\frac{d\phi_{Sol,Test}}{dx}$ is a test potential gradient that corresponds the potential change V_{max} and a charge density $q_{Sol,Test}$ contained within a close-packed structure made up of hydrated ions.
- $\frac{d\phi_{Solution}}{dx}$ corresponds to the potential difference *V10-V9* calculated from standard procedure where $q_{Solution}$ is calculated by finding the equilibrium between the solid and the solution.

Our test potential gradient is given by

$$\frac{d\phi_{Sol,Test}}{dx} = -\left\{\frac{2kT}{\varepsilon_{Solution}\varepsilon_0}\left[\sum_i (n_i^0 - 1)e^{\left(\frac{-z_i\, e\, Vmax}{kT}\right)}\right]\right\}^{\frac{1}{2}} \quad \text{(S29)}$$

And the corresponding charge density

$$q_{Sol,Test} = \frac{-(V10 - V9)}{|V10 - V9|}\left(\frac{d\phi_{Sol,Test}}{dx}\right)\varepsilon_{Solution}\varepsilon_0 \tag{S30}$$

where $\frac{-(V10-V9)}{|V10-V9|}$ gives the charge sign of the majority hydrated ion that accumulates at the interface to form the Stern layer. The resultant charge density in the Stern layer is given by

$$\sigma^S = q_{Sol,Test} - q_{Solution} \tag{S31}$$

We may approximate the thickness of the Stern layer by assuming that the volumetric charge density throughout the Stern layer is equal to that at V_{max} which occurs at distance x^S such that

$$\sigma^S = x^S\,\rho(x = x^S) = x^S \sum_i n_i^0\, z_i\, e \exp\left(\frac{-z_i\, e\, V_{max}}{kT}\right) \tag{S32a}$$

Or

$$x^S = \frac{\sigma^S}{\sum_i n_i^0\, z_i\, e \exp\left(\frac{-z_i\, e\, V_{max}}{kT}\right)} \tag{S32b}$$

In the case of Figure 7 of the manuscript and **Figure S9**, the calculated charge densities and potentials for the p-type semiconductor/insulator/solution junction did not require the use of a Stern layer. This is a point of caution for readers planning on using this section and **Section 6 in the manuscript** to investigate electrochemical electrode interfaces.

End of step for invoking a Stern layer

Like with the solid state junctions discussed in the early sections of the manuscript, we also produce energy band diagrams for the p-type semiconductor/insulator/solution junction. As we only provide potential profiles within the manuscript, we provide the energy band diagrams here (Figure S9):

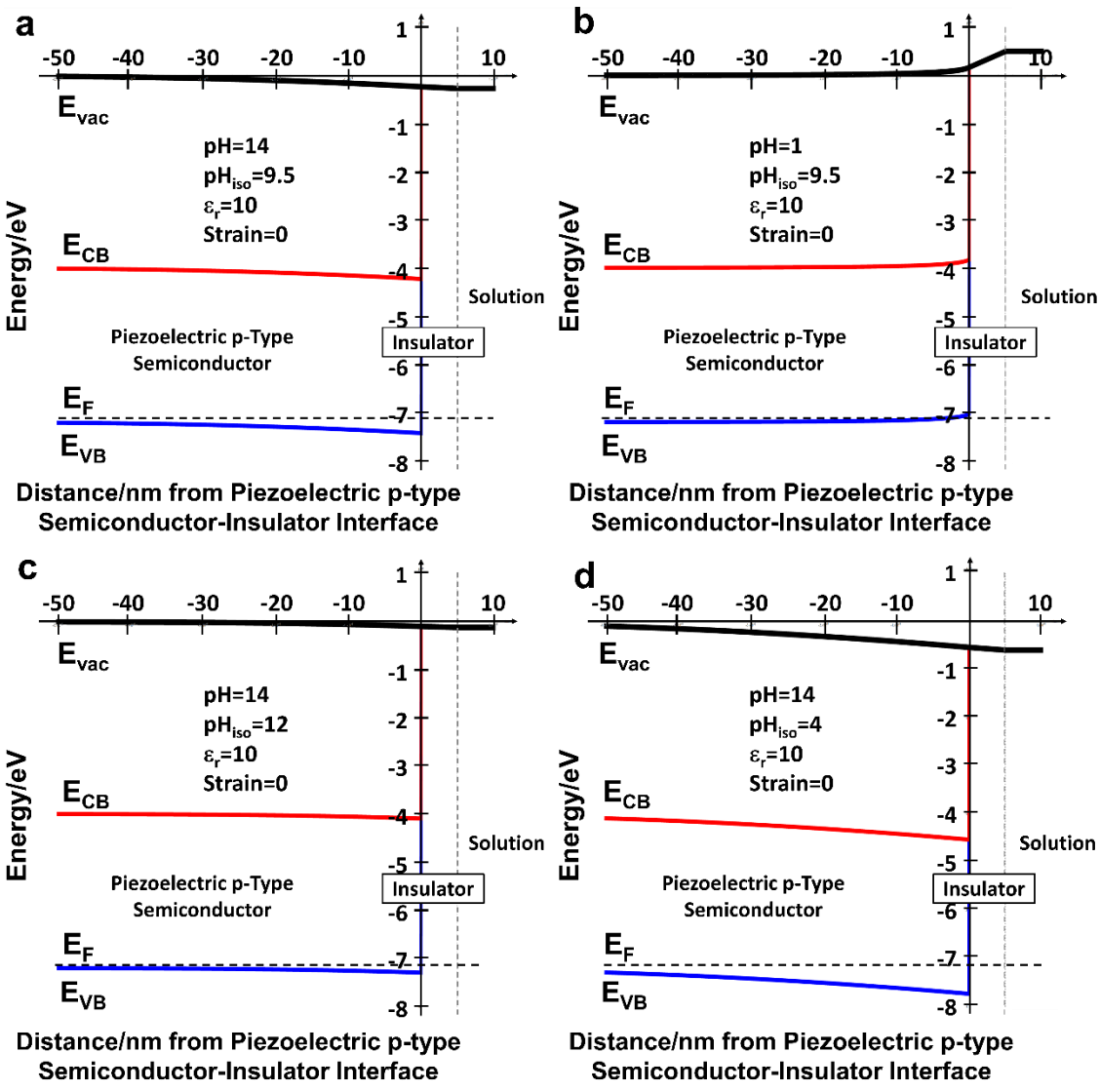
a
b
c
d
E_vac
E_CB
E_F
E_VB
pH=14
pH_iso=9.5
ε_r=10
Strain=0
pH=1
pH_iso=9.5
ε_r=10
Strain=0
pH=14
pH_iso=12
ε_r=10
Strain=0
pH=14
pH_iso=4
ε_r=10
Strain=0
Piezoelectric p-Type Semiconductor
Insulator
Solution
Energy/eV
Distance/nm from Piezoelectric p-type Semiconductor-Insulator Interface

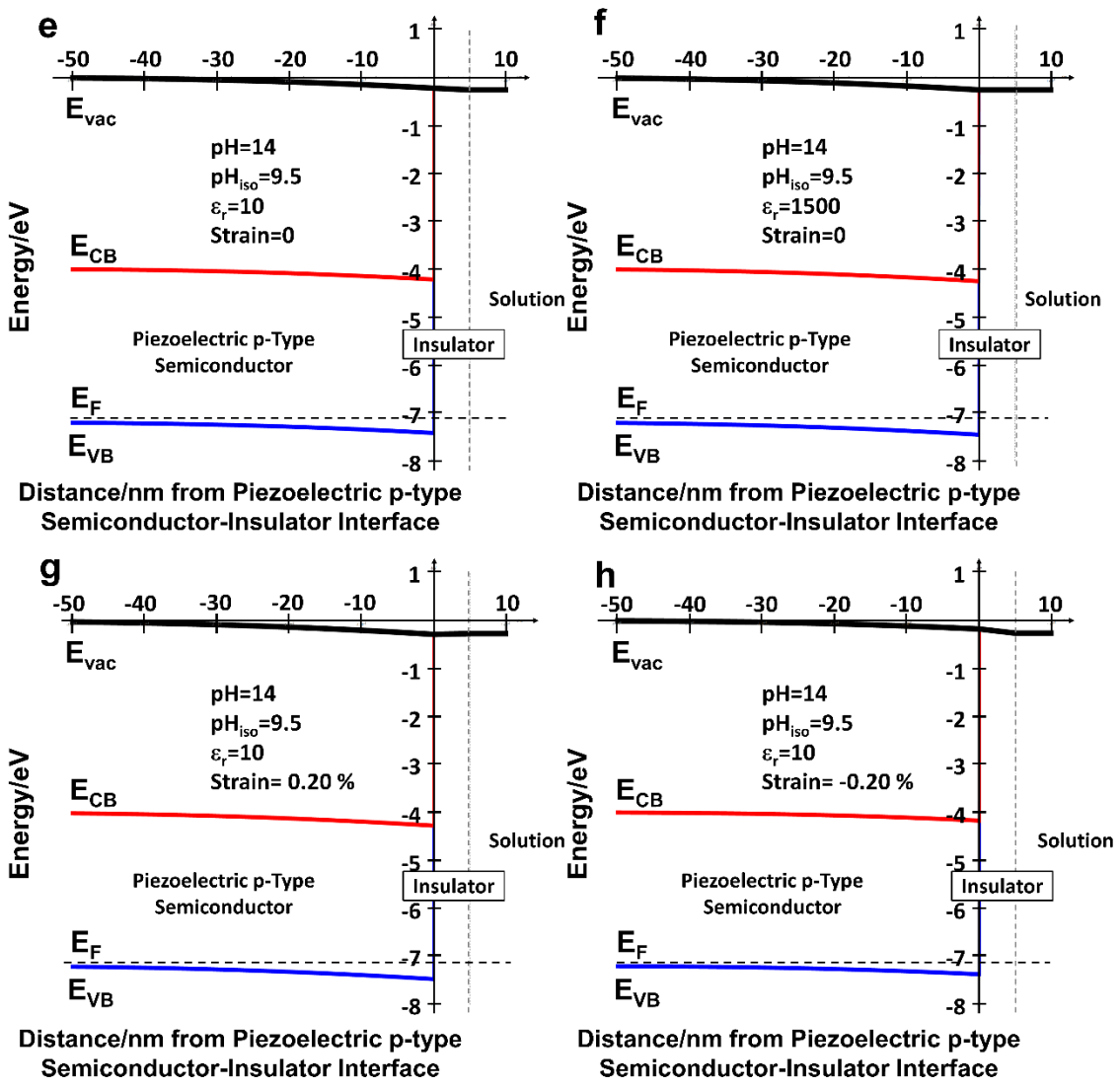

Figure S9. Equilibrium energy band diagrams for p-type semiconductor/insulator/solution junction. a. and **b.** the effect of *pH* with constant pH_{iso}. **c.** and **d.** the effect of pH_{iso} with constant *pH*. **e.** and **f.** the effect of changing the relative electrical permittivity ε_r of the insulator. **g.** and **h**. the effect of piezoelectric charge. Note that g. and h.—like previously discussed junctions that include piezoelectric junctions with an intermediate insulator—involve an insulator with a small relative electrical permittivity. High relative electrical permittivities require larger accumulation of charge on either side of the dielectric, thus the effect of piezoelectric polarization depreciates with increasing relative electrical permittivity of the intermediate insulator.

References:

[1] T. Tiedje, C. Wronski, J. Cebulka, *J. Non-Cryst. Solids* **1980**, *35–6*, 743.

[2] I. Hiromitsu, G. Kinugawa, *Jpn. J. Appl. Phys. Part 1-Regul. Pap. Brief Commun. Rev. Pap.* **2005**, *44*, 60.

[3] A. G. Pattantyus-Abraham, I. J. Kramer, A. R. Barkhouse, X. Wang, G. Konstantatos, R. Debnath, L. Levina, I. Raabe, M. K. Nazeeruddin, M. Graetzel, E. H. Sargent, *Acs Nano* **2010**, *4*, 3374.

[4] K. W. Johnston, A. G. Pattantyus-Abraham, J. P. Clifford, S. H. Myrskog, S. Hoogland, H. Shukla, E. J. D. Klem, L. Levina, E. H. Sargent, *Appl. Phys. Lett.* **2008**, *92*, 122111.

[5] L. Hong-Xia, G. Bo, Z. Qing-Qing, W. Yong-Huai, *Acta Phys. Sin.* **2012**, *61*, 057802.

[6] S. M. Sze, Ng, Kwok K., *Physics of Semiconductor Devices*, John Wiley And Sons, Hoboken, NJ, **2007**.

[7] C. C. Hu, *Modern Semiconductor Devices for Integrated Circuits*, Pearson, Upper Saddle River, N.J, **2009**.

[8] J. Kielland, *J. Am. Chem. Soc.* **1937**, *59*, 1675.